

Sl. No.	<p style="text-align: center;"><b>IIT Ropar</b>  <b>List of Recent Publications with Abstract</b>  <b>Coverage: July, 2020</b></p>
1.	<p><a href="#"><u>A C3-symmetrical tripodal acylhydrazone organogelator for the selective recognition of cyanide ions in the gel and solution phases: practical applications in food samples</u></a>  S Sharma, M Kumari, N Singh - <i>Soft Matter</i>, 2020</p> <p><b>Abstract:</b> The method of formation of low-molecular-weight organogelators via modifications in the substituents has been demonstrated. The organogelator formed can selectively sense cyanide ions in the gel and solution phases. Interaction of cyanide with acylhydrazone was noticeably visible to the “naked eye” and was proved using <sup>1</sup>H NMR titrations. Notably, the ligand has been successfully explored for the recognition of cyanide ions in food samples. Additionally, low-cost cotton swabs coated with the organogelator showed rapid, on-site recognition of cyanide ions. The structure–property relationship discovered in the given study provides insight into the development of novel, cost-effective multifunctional materials.</p>
2.	<p><a href="#"><u>A low-cost device for rapid 'color to concentration' quantification of cyanide in real samples using paper-based sensing chip</u></a>  H Singh, G Singh, DK Mahajan, N Kaur, N Singh - <i>Sensors and Actuators B: Chemical</i>, 2020</p> <p><b>Abstract:</b> Highly selective azophenol-based chromogenic probe was synthesized that gave sharp color change in presence of cyanide. Based on colorimetric response of probe, a simple and economic colorimetric device has also been developed. Recently smartphones were employed for colorimetric analysis however there are number of limitations associated with it. Therefore, colorimeter was built using color sensor (TCS3200) and Arduino microcontroller for quantification of analytes using sensor coated paper chip. Initial colorimetric experiments revealed that sensor coated paper chip gave most linear response for change in the intensity of green component with change in the concentration of the cyanide. Thus, the device was calibrated using sensor coated paper chip and known concentrations of cyanide. It produced a best linear response over the range of 0–20 μM concentration of cyanide with R<sup>2</sup> value of 0.9858 and limit of detection was calculated to be 0.86 μM which is lesser than WHO’s permissible limit of 1.9 μM. Finally, the applicability of device was successfully evaluated for quantification of cyanide concentration in spiked river water and food samples. Thus, the device can be successfully calibrated and used for quantitative analysis of other hazardous analytes such as cyanide through colorimetric sensing chips.</p>
3.	<p><a href="#"><u>A Machine Learning Approach to Carotid Wall Localization in A-mode Ultrasound</u></a>  S Singh, AK Sahani - <i>IEEE International Symposium on Medical Measurements and Applications (MeMeA)</i>, 2020</p> <p><b>Abstract:</b> ARTSENS is being developed as a fully automated ultrasound based imageless system to facilitate mass screening of patients for early detection of atherosclerosis especially in low- and middle- income countries. ARTSENS uses a single element ultrasound transducer and thus makes its measurement on basis of observations on A-line. Positioning the single element transducer on the carotid artery and automatic identification of proximal and distal walls are a major challenge in this device. In this paper, we explore various machine learning methods namely – logistic regression, support vector machine and Adaboost, on selectively extracted features. The algorithms were trained on data from 60 subjects and tested on data from 40 subjects. Adaboost algorithm performed the best among the three logging a 91.66% accuracy.</p>

4.	<p><a href="#">A Multi-application Compact Ultra Wideband Vivaldi Antenna for IoT, 5G, ITS, and RFID</a> M Kumar, S Agarwal, A Sharma - IEEE Indian Conference on Antennas and Propagation, 2019</p> <p><b>Abstract:</b> A miniaturized wideband Vivaldi antenna is presented in this paper. The proposed antenna is compact in size, has wide bandwidth and high radiation efficiency. The proposed antenna is simulated and fabricated on FR-4 substrate with overall dimensions of <math>20 \times 17</math> mm<sup>2</sup>. The resonating frequency of the reported design is observed as 5.8GHz and impedance bandwidth is 2.67GHz (4.94GHz - 7.61GHz). The simulated radiation efficiency and gain are approximately 98.9% and 3.66dBi, respectively. The proposed design finds its applications in IoT, 5G, Wireless LAN (WLAN), Intelligent Transportation System (ITS) and Radio Frequency Identification (RFID).</p>
5.	<p><a href="#">A Temperature and Dielectric Roughness-Aware Matrix Rational Approximation (MRA) Model for the Reliability Assessment of Copper-Graphene Hybrid On-Chip Interconnects</a> R Kumar, A Kumar, S Guglani, S Kumar, S Roy.... R Sharma... - IEEE Transactions on Components, Packaging and Manufacturing Technology, 2020</p> <p><b>Abstract:</b> In this paper, a closed-form matrix rational approximation (MRA) model is presented for the reliability assessment of copper-graphene hybrid on-chip interconnect networks. The key feature of this MRA model is its capacity to predict how different values of temperature and dielectric roughness affect the signal integrity performance of the hybrid interconnect networks. As a result, the proposed MRA model is well-suited for very fast parametric sweeps and worst-case analysis of the hybrid interconnect networks, which has not been possible using existing closed-form models or even SPICE simulations. Numerical examples show that the proposed model is significantly more efficient than conventional models while exhibiting error less than 5%.</p>
6.	<p><a href="#">An algebraic method of solution of a water wave scattering problem involving an asymmetrical trench</a> A Kaur, SC Martha, A Chakrabarti - Computational and Applied Mathematics, 2020</p> <p><b>Abstract:</b> The problem of propagation of obliquely incident surface water waves involving an asymmetric rectangular trench in a channel of finite depth is examined for its solution. The problem under consideration leads to multiple series relations involving trigonometric functions. Instead of converting these relations into systems of integral equations, direct algebraic approaches are utilized and the corresponding solutions are obtained approximately, by way of solving the reduced system of over-determined algebraic equations. The system of over-determined algebraic equations are solved with the aid of the well-known algebraic approaches “Least square” (LS) and “Singular value decomposition” (SVD) methods. The presently determined results involving the reflection and transmission coefficients related to the scattering problem under consideration, agree very well, with the known results obtained recently, where integral equations and their approximate numerical solutions were determined. The effect of system of parameters on hydrodynamics quantities such as reflection and transmission coefficients, wave elevation are analysed and shown through tables and graphs. The present algebraic methods appear to be very direct and quick. A similar techniques are found to be applicable to the problem of scattering of surface water waves by any finite number of asymmetrical placed rectangular trenches. The problem of a pair of asymmetrical trenches is under progress. The energy balance relation for the given problem is derived and used to check the accuracy of numerical results. Some important results such as wave elevation profiles, the singularity behaviour of the flow near trench edges are investigated and analyzed through graphs.</p>

[Bank competition in India: revisiting the application of Panzar–Rosse model](#)

B Rakshit, S Bardhan - Managerial Finance, 2020

**Abstract:**

Purpose

The paper measures the degree of bank competition in Indian banking over the period 1996–2016. Using bank-level annual data, we revisit the case of banking competitiveness during the prefinancial and postfinancial crisis and examine whether the global financial crisis alters the level of bank competition in India. Additionally, this paper addresses the misspecification issues associated with the widely used Panzar–Rosse model in Indian banking context.

Design/methodology/approach

We apply Panzar and Rosse (1987) H-statistic and evaluate the degree of bank competition by estimating the extent to which changes in input prices are reflected in revenues earned by banks. Subsequently, we link this measure of competitiveness to a number of structural indicators (HHI and CRn) to examine the structure-conduct-performance hypothesis, which assumes that a concentrated banking system can impair competition. The simple panel regression model was used to handle the empirical estimations.

Findings

7. findings reveal that the Indian banking system operates under competitive conditions and earns revenues as if under the monopolistic competition. We also find evidence that Indian banks are competitive, even under a concentrated market structure. This observation runs, in contrary, to the prediction of the structure–conduct–performance hypothesis. The findings also indicate the differences in the estimated H-statistic value after considering the misspecifications of the P–R model.

Practical implications

From policy perspectives, policymakers should focus more on maintaining an optimal level of bank competition by mitigating entry restrictions, exercising less consolidation and withdrawing overregulation from banking activities. A competitive banking industry ensures both efficiency and stability.

Social implications

A competitive banking sector by lowering interest rates margin provides easier access to finance to both households and small and medium enterprises (SMEs).

Originality/value

This is the only study that addresses the misspecification of the P–R model while assessing competition in Indian banking and provides a thorough understanding of the role of concentration on bank competition.

[Bi-Functional Magnesium Silicate Catalyzed Glucose and Furfural Transformations to Renewable Chemicals](#)

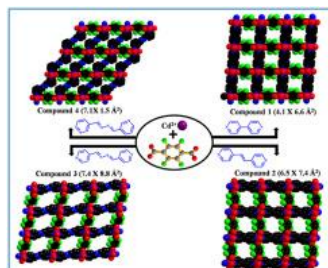
R Srivastava, A Kumar – ChemCatChem, 2020

8. **Abstract:** Bio-refinery is attracting significant interest to produce a wide range of renewable chemicals and fuels from biomass that are alternative to fossil fuel derived petrochemicals. Similar to petrochemical industries, bio-refinery also depends on solid zeolite catalysts. Acid-base catalysis plays pivotal role in producing a wide range of chemicals from biomass. Herein, the Mg framework substituted MTW zeolite is synthesized and explored in the valorization of glucose and furfural. Bi-functional (acidic and basic) characteristics are confirmed using pyridine adsorbed FT-IR analysis and NH<sub>3</sub> and CO<sub>2</sub> temperature-programmed desorption techniques. Textural properties and morphological information are retrieved from N<sub>2</sub>-sorption, X-ray photoelectron spectroscopy, and electron microscopy. The activity of the catalyst is demonstrated in the selective isomerisation of glucose to fructose in ethanol.

	<p>Glucose is converted to methyl lactate in high yield using the same catalyst. Further, the bi-functional activity of this catalyst is demonstrated in the production of fuel precursor by the reaction of furfural and isopropanol. Mg-MTW zeolite exhibits excellent activity in the production of all these chemicals and fuel derivative. The catalyst exhibits no significant loss in the activity even after five recycles. One simple catalyst affording three renewable synthetic intermediates from glucose and furfural will attract significant attention to catalysis researchers and industrialists.</p>
9.	<p><a href="#">Blind Cancellation in Radar Based Self Driving Vehicles</a> R Singh, D Saluja, S Kumar - IEEE Transactions on Vehicular Technology, 2020</p> <p><b>Abstract:</b> Mutual interference among the radar sensors has become a serious concern due to the extensive growth of self driving vehicles (SDV) equipped with such sensors. The problem becomes more severe with the increase in traffic density, where a large number of SDVs gather within the proximity of inter-vehicular radars. Thereby, the number of resources required to maintain the neighbourhood orthogonality increases with traffic density and further leads to the problem of radar blindness. In this paper, we propose a graph-based resource allocation (GRA) scheme to assign resources to the running SDV pool. GRA assures that two closely located SDVs may not simultaneously use the same resource. Also, we integrate the notion of traffic-based dynamic-range approach (TDA) with GRA. Then, through simulation results, it is shown that GRA outperforms the state of art random allocation approach. Further, it is shown that GRA, along with TDA, may eliminate the problem of radar blindness.</p>
10.	<p><a href="#">Comprehensive Understanding of the Eco-friendly Synthesis of Zeolites: Needs of 21st Century Sustainable Chemical Industries</a> P Rani, R Srivastava - The Chemical Record, 2020</p> <p><b>Abstract:</b> Zeolites have taken a leading position in petrochemical, fine, and bulk chemical industries due to their porous architecture, pore sizes, tunable acidity, and thermal stability. Various strategies of zeolites preparation, including template-free, solvent-free, and toxic mineral-free strategies are summarized. Moreover, the zeolite synthesis using naturally occurring minerals and sustainable natural templates is also discussed, which involves the synthesis of nanocrystalline zeolites of different framework structures using plant-based natural templates and biomass-derived renewable chemicals. Overall this personal account provides the fundamentals of various sustainable synthetic strategies reported in the literature for the synthesis of zeolites with suitable examples that will be useful for the students and will motivate experienced researchers to develop various novel sustainable methods for the synthesis of zeolites and other inorganic materials of industrial relevance.</p>
11.	<p><a href="#">Construction of highly water-stable fluorinated 2D coordination polymers with various N, N'-donor: Syntheses, crystal structures and photoluminescence properties</a> SS Dhankhar, CM Nagaraja - Journal of Solid State Chemistry, 2020</p> <p><b>Abstract:</b> Four new 2D coordination polymers (CPs) of Cd(II), [Cd(tfbdc)(bpy)(H<sub>2</sub>O)<sub>2</sub>]<sub>n</sub> (1) [Cd(tfbdc)(bpe)(H<sub>2</sub>O)<sub>2</sub>]<sub>n</sub> (2), [Cd(tfbdc)(4bpdb)(H<sub>2</sub>O)<sub>2</sub>]<sub>n</sub> (3), and [Cd(tfbdc)(3bpdb)(H<sub>2</sub>O)<sub>2</sub>]<sub>n</sub> (4) (where, tfbdc = 2,3,5,6-tetrafluoro-1,4-benzenedicarboxylate, bpy = 4,4'-bipyridine, bpe = 1,2-bis(4-pyridyl)ethylene, 4bpdb = 1,4-bis(4-pyridyl)-2,3-diaza-1,3-butadiene), and 3bpdb = 1,4-bis(3-pyridyl)-2,3-diaza-1,3-butadiene) were successfully synthesized by room temperature self-assembly of Cd(II), tfbdc<sup>2-</sup> and the N, N'-bipyridine linkers. All four CPs were thoroughly characterized by single-crystal X-ray diffraction and other physicochemical studies. Structural analysis revealed that CPs 1–4 feature a 2D network structure which is further extended to 3D</p>

supramolecular framework via intermolecular (O–H···O) hydrogen bonding interactions between the hydrogens of the coordinated water molecule and the free carboxylate oxygen of tfbdc2– dianion. Further, the use of various ancillary bipyridine linkers has resulted in the 2D networks 1–4 with different pore sizes. Interestingly, 1–4 exhibit water stability owing to the presence of fluorinated aromatic dicarboxylate ligand and also, photoluminescence emission attributed to intra-ligand and/or ligand-to-ligand charge transfer transitions.

**Graphical Abstract:**



12.

[Design of Active Common Mode Noise Voltage Canceler for SiC Inverter Fed Induction Motor Drive with Reduced Common Mode Voltage PWM](#)

M Kumar, K Jayaraman - 2020 IEEE 29th International Symposium on Industrial Electronics, 2020

**Abstract:** This paper presents the design of active common mode noise voltage canceler (ACVC) for induction motor drive with active zero vector pulse width modulation (AZPWM-1). Conventional pulse width modulation (PWM) like space vector pulse width modulation (SVPWM) has a peak to peak (PP) value of common mode voltage (CMV) equal to the DC link voltage. Compared to conventional PWM, AZPWM-1 reduces the PP value of CMV by three times. This leads to reduction in magnetizing inductance of common mode transformer (CMT) and ratings of components used in ACVC. The aforementioned modification in ACVC improves the electromagnetic interference (EMI) performance, reduce the peak value of CMV and ground current with lower magnetizing inductance of CMT.

13.

[Development of Ionic Liquid@ Metal Based Nanocomposites-Loaded Hierarchical Hydrophobic Surface to the Aluminium Substrate for Antibacterial Properties](#)

D Bains, G Singh, N Kaur, N Singh - ACS Applied Bio Materials, 2020

**Abstract:** Designing biomaterials and substrates possessing antibacterial properties is a growing field nowadays. In this context, we have developed benzimidazolium ionic liquids ILs-1(a–d)-based metal hybrid nanocomposites using various metals such as silver (Ag), gold (Au), and copper (Cu), which were fully characterized by various techniques. Their morphology, elemental composition, crystallinity, and size were studied by scanning electron microscopy (SEM), energy-dispersive X-ray spectroscopy, powder X-ray diffraction, and dynamic light scattering, respectively. Further, the prepared ionic liquids ILs-1(a–d) and ionic liquid@metal composites were screened for their antibacterial potential against Gram-positive and Gram-negative pathogenic microorganisms via the colony forming unit assay, and their minimum inhibitory concentrations (MICs) were also evaluated. The results obtained from preliminary antibacterial screening demonstrated that these ionic liquid@metal nanocomposites IL-1d@M (M = Ag, Cu, and Au) exhibited potent antibacterial activity in comparison to the ionic liquids ILs-1(a–d). In particular, the ionic liquid@silver nanocomposites (IL-1d@Ag) showed the most potent activity against both E. coli and S. aureus bacterial strains with MIC = 12 ± 2 and 08 ± 2 µg/mL, respectively. The mechanism of action for antibacterial activity of IL-1d@Ag nanocomposites was



	<p>investigated through generation of 1O2 (ROS), whereas the morphology of treated pathogenic bacteria was examined through atomic force microscopy and SEM. Furthermore, to utilize this developed material IL-1d@Ag in biomedical applications, the prepared ionic liquid material was fabricated onto a microstructured aluminum (Al) substrate with hierarchically arranged functionalities, and the modified surface was characterized and also evaluated for antibacterial activity. Moreover, the hydrophobicity of the material coated onto the Al substrate was also measured by static water contact angle measurement, which reveals its improved hydrophobic character. Thus, the developed hierarchical hydrophobic coating material possessing long-term antibacterial activity on an Al substrate may minimize the wetting by biological secretions and also prevent the substrate from corrosion.</p>
14.	<p><a href="#"><u>Development of magnesium-based hybrid metal matrix composite through in situ micro, nano reinforcements</u></a>  H Singh, D Kumar, H Singh - Journal of Composite Materials, 2020</p> <p><b>Abstract:</b> Present work aims at developing Magnesium based metal matrix composite (MMC) through in-situ reaction. In-situ generation of micro and nano particles in the Mg-melt is supposed to have a better bonding with the matrix. Ceric ammonium nitrate (CAN) is added to initial Magnesium melt (with an aim to generate CeO<sub>2</sub> and MgO through in-situ reaction) at temperatures of 670 °C and 870 °C. The developed MMCs are solution treated to get rid of intermetallic. The nature of particles is explored with X-ray diffraction (XRD) and Energy dispersion spectroscopy (EDS). The morphology and sizes of particles are keenly jotted using scanning electron microscope (SEM). Mechanical responses of developed MMCs are recorded through Hardness, Compression and scratch tests. The compression fractured surfaces are analyzed with SEM and scratched samples are analyzed on 3 D optical profilometer to explore deformation behavior. The observations indicate the in-situ formation of CeO<sub>2</sub>, MgO and CeMg<sub>12</sub> intermetallic phases in different types and sizes. Further, these particles are responsible for improved mechanical properties. The findings are supported by the contribution of different strengthening mechanisms.</p>
15.	<p><a href="#"><u>Does Bank Competition Enhance or Hinder Financial Stability? Evidence from Indian Banking</u></a>  B Rakshit, S Bardhan - Journal of Central Banking Theory and Practice, 2020</p> <p><b>Abstract:</b> The primary purpose of this paper is to empirically investigate the impact of bank competition on financial stability in India. We use a dynamic panel model to examine whether an increase in bank competition hinders financial stability of commercial banks in India over the period 1996 to 2016. Findings reveal that in India, a higher degree of bank competition is positively associated with the prevalence of non-performing loans. Additionally, the positive impact of the Lerner index on Z-score lends support to competition-fragility hypothesis. However, we argue that both the views of competition-stability and competition-fragility can coexist in a single banking system like India.</p>
16.	<p><a href="#"><u>Does higher educational attainment imply less crime? Evidence from the Indian states</u></a>  B Rakshit, Y Neog - Journal of Economic Studies, 2020</p> <p><b>Abstract:</b>  Purpose  The primary purpose of this paper is to empirically investigate the impact of educational attainment on crime rates across 33 Indian states over the period 2001 to 2013. This paper also examines the role of various macroeconomic, socio-economic and demographic factors in determining the variation of crimes in India.  Design/methodology/approach</p>

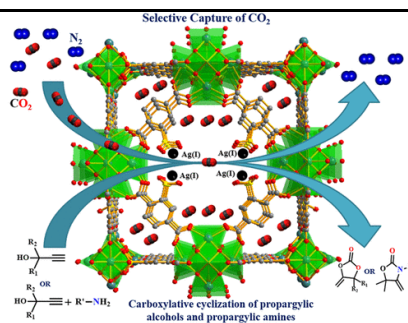
	<p>First, this paper provides a representative theoretical model and discusses the possible relationship between crime and education. Second, the paper applies a dynamic panel data (DPD) model to extract more precise, unbiased and reliable estimates of the effect of education in abating different crime rates. The main advantage of using the dynamic panel model is to address the problem of endogeneity in some regressors and capture the time persistent effect of education on crime.</p> <p><b>Findings</b> Empirical findings reveal that a 1% increase in gross enrolment ratio leads to the reduction of total crime by 8%. However, a unique finding identifies a positive association between tertiary education and economic crime. This finding further goes against the general belief that criminals tend to be less educated than non-criminals.</p> <p><b>Practical implications</b> This paper recommends that instead of punishment and mandatory law enforcement for offenders, increase in government expenditure and different educational attainment ratios can go a long way to combat crime in India, which has posed a serious threat to the stability of society. Furthermore, utilizing the information on offenders' educational attainment in examining the crime rates can be a future research agenda for policymakers.</p> <p><b>Originality/value</b> This study contributes to the empirical debate of 'crime-education nexus' by examining the role of education on crime in India. This study is the first of its kind that focuses on the aspects of crime and education more recently and investigates the relationship between crime and education due to the recent changes in educational attainment ratios and crime rate.</p>
17.	<p><a href="#"><u>Does trade openness affect economic growth in India? Evidence from threshold cointegration with asymmetric adjustment</u></a> L Mallick, SR Behera - Cogent Economics &amp; Finance, 2020</p> <p><b>Abstract:</b> This paper investigates the long-run equilibrium relationship between economic growth and trade openness in India during the period 1960–2018 using the asymmetric error-correction model with threshold cointegration. To evaluate the robustness impact of trade openness on economic growth under different regimes, we divide the full sample period into two sub-periods, i.e., pre-trade reforms period 1960–1990, and post-trade reforms period 1991–2018. The study indeed confirms the evidence of asymmetric cointegration between economic growth and trade openness in India during the period under evaluation and over the different sub-periods. The estimated asymmetric error-correction model exhibits a different speed of adjustment in trade openness in response to positive and negative economic growth shocks in the short-run. More specifically, during the pre-reforms period, deviations from the long-run equilibrium due to a relative increase in economic growth have a lower speed of adjustment in comparison to deviations caused by a corresponding decrease in economic growth in India.</p>
18.	<p><a href="#"><u>Effect of device dimensions, layout and pre-gate carbon implant on hot carrier induced degradation in HKMG nMOS Transistors</u></a> P Duhan, VR Rao, NR Mohapatra - IEEE Transactions on Device and Materials Reliability, 2020</p> <p><b>Abstract:</b> The hot carrier (HC) induced degradation has become a major concern in advanced CMOS technologies because of non-scalable VDD. In this work, we have shown that the HC induced degradation in gate-first HKMG nMOS transistors can be modulated by optimizing the device width, lanthanum capping layer thickness, and pre-gate carbon (C) implant. The physics responsible for these observations are investigated and attributed to the reduction in the number of defects (traps) in hafnium oxide (HfO<sub>2</sub>) and reduction in carrier injection into</p>

	<p>these defects. It is also shown that the HC performance of these transistors could be further improved by increasing the active-to-active spacing.</p>
19.	<p><a href="#">Efficient Electro-Mechanical Conversion System in Bladeless Wind Turbines</a>  A Gautam, SS Srinivas, AVR Teja - IEEE 29th International Symposium on Industrial Electronics, 2020</p> <p><b>Abstract:</b> Vortex bladeless wind turbines generate electrical power from vibration unlike conventional wind turbines where rotary motion is converted to electrical energy. For achieving maximum electrical output in the bladeless turbine for a given vibration, the design of the electro-mechanical conversion system is critical. In this paper, different possible arrangements of the field with respect to the coil to harness electrical power are discussed in detail and an efficient arrangement was proposed for maximum voltage generation. All the propositions are thoroughly analyzed using Ansys and typical results are presented.</p>
20.	<p><a href="#">Exceptionally Plastic/Elastic Organic Crystals of a Naphthalidenimine-Boron Complex Show Flexible Optical Waveguide Properties</a>  K Naim, M Singh, S Sharma, R Nair, P Venugopalan... - Chemistry–A European Journal, 2020</p> <p><b>Abstract:</b> Design of molecular compounds exhibiting flexibility is an emerging area of research. Although a fair amount of success has been achieved in the design of plastic or elastic crystals, realizing multi-dimensional plastic and elastic bending remains challenging. We report herein a naphthalidenimine-boron complex that showed size-dependent dual mechanical bending behavior whereas its parent Schiff base was observed to be brittle. Detailed crystallographic and spectroscopic analysis revealed the importance of boron in imparting the interesting mechanical properties. Further, the luminescence of the molecule was turned-on subsequent to boron complexation thereby allowing it to be explored for multi-mode optical waveguide applications. Our in-depth study of the size-dependent plastic and elastic bending of the crystals thus provides important insights in molecular engineering and could act as a platform for the development of future smart flexible materials for optoelectronic applications.</p>
21.	<p><a href="#">Exploring Sustainability in Indian Pharmaceutical Industry</a>  M Sharma, U Chaturvedi, GS Dangayach, P Sarkar - Enhancing Future Skills and Entrepreneurship: Part of the Sustainable Production, Life Cycle Engineering and Management book series, 2020</p> <p><b>Abstract:</b> Use of technology in this era requires organizational goals to be met more than just maximizing profit and capturing more and more market share. The aim of this research is to explore sustainability awareness in Indian pharmaceutical industry by considering social well-being along with economic and environmental aspects and attainment of key drivers. Despite moving towards 21st century, it is a fact that sustainability and related practices in Indian pharmaceutical industry is still in its infancy. Thus, looking at sustainability comprehensively, its awareness and related practices needs to be explored by incorporating them at strategic, tactical and operational level functions of a pharmaceutical organization. Once these aspects are explored, this will not only help to improve the environmental performance of an organization but also enhance managerial capability and decision-making capacity. This work has been carried out as a part of an ongoing research to identify and establish theoretical relationship between sustainability awareness, triple bottom line and key drivers. Therefore, it is expected that its practical implementation can be achieved in future with greater clarity.</p>



22.	<p><a href="#">Flow and thermal characteristics of two interacting cylinders in the yield stress fluid</a>  S Gupta, SA Patel, RP Chhabra - <i>Computational Thermal Sciences: An International Journal</i>, 2020</p> <p><b>Abstract:</b> In this work, steady and laminar flow of a viscoplastic fluid past two circular cylinders in a tandem arrangement has been investigated numerically. The governing differential equations for a Bingham model fluid have been solved over wide ranges of conditions as: Bingham number (<math>0.01 \leq Bn \leq 100</math>), Reynolds number (<math>0.01 \leq Re \leq 40</math>) and Prandtl number (<math>10 \leq Pr \leq 100</math>) in order to delineate the influence of each of these parameters on the momentum and heat transfer characteristics. In addition, the severity of the interactions between the two cylinders was varied by varying the center-to-center distance between the two cylinders in the range <math>2 \leq G \leq 10</math>. Detailed results in terms of the streamlines, isotherm contours, yielded/unyielded regions, shear rate profiles, local Nusselt number, in the vicinity of the cylinder have been discussed here. Further detailed insights are developed in terms of the distribution of velocity along the lines of symmetry. Finally, the overall behaviour is captured in terms of drag coefficient and the average Nusselt number as functions of the pertinent governing parameters namely, <math>Bn</math>, <math>Re</math>, <math>Pr</math> and <math>G</math>. To facilitate the estimation of drag and Nusselt number (in terms of <math>j</math> factor) in a new application, the present numerical results have been consolidated in terms of predictive equations as functions of the pertinent dimensionless parameters. The present results reveal a significant impact of interactions between the cylinders, i.e., gap ratio on the detailed flow and thermal patterns and the overall characteristics.</p>
23.	<p><a href="#">From pyramids to state-of-the-art: a study and comprehensive comparison of visible–infrared image fusion techniques</a>  AM Sharma, A Dogra, B Goyal, R Vig, S Agrawal - <i>IET Image Processing</i>, 2020</p> <p><b>Abstract:</b> Image fusion has emerged as a major area of research in the past few decades due to its extended applications. While progressing in the field of image fusion, a large number of techniques-based image transforms and spatial filters have been devised for both general and specific sets of images. The primary criterion of image fusion technique is to deliver high-quality visual perception besides giving a considerable objective evaluation rate. In this study, an information fusion rate-based study is done on recent, most researched, and high-performing state-of-the-art techniques using visible and infrared image datasets. These techniques have been chosen carefully, owing to their superiority in performance on both objective and subjective scales of evaluation and have been discussed in terms of their respective advantages and disadvantages. It is clearly evident that some rather primitive techniques can perform well as well as techniques based on a hybrid of various domains can significantly boost the information fusion rate.</p>
24.	<p><a href="#">Gordian complexes of knots and virtual knots given by region crossing changes and arc shift moves</a>  A Gill, M Prabhakar, A Vesnin - <i>Journal of Knot Theory and its Ramifications</i>, 2020</p> <p><b>Abstract:</b> Gordian complex of knots was defined by Hirasawa and Uchida as the simplicial complex whose vertices are knot isotopy classes in <math>S^3</math>. Later Horiuchi and Ohyama defined Gordian complex of virtual knots using <math>v</math>-move and forbidden moves. In this paper we discuss Gordian complex of knots by region crossing change and Gordian complex of virtual knots by arc shift move. Arc shift move is a local move in the virtual knot diagram which results in reversing orientation locally between two consecutive crossings. We show the existence of an arbitrarily high dimensional simplex in both the Gordian complexes, i.e., by region crossing change and by the arc shift move. For any given knot (respectively, virtual knot)</p>

	<p>diagram we construct an infinite family of knots (respectively, virtual knots) such that any two distinct members of the family have distance one by region crossing change (respectively, arc shift move). We show that that the constructed virtual knots have the same affine index polynomial.</p>
25.	<p><a href="#">High temperature behavior of non-local observables in boosted strongly coupled plasma: A holographic study</a>  A Bhatta, S Chakraborty, S Dengiz... - The European Physical Journal C, 2020</p> <p><b>Abstract:</b> In this work, we perform a holographic analysis to study non local observables associated to a uniformly boosted strongly coupled large N thermal plasma in d-dimensions. In order to accomplish the holographic analysis, the appropriate dual bulk theory turns out to be d+1 dimensional boosted AdS-Schwarzschild blackhole background. In particular, we compute entanglement entropy of the boosted plasma at high temperature living inside a strip geometry with entangling width l in the boundary at a particular instant of time. We also study the two-point correlators in the boundary by following geodesic approximation method. For analyzing the effect of boosting on the thermal plasma and correspondingly on both non local observables, we keep the alignment of the width of region of interest both parallel and perpendicular to the direction of the boost. We find our results significantly modified compared to those in un-boosted plasma up to the quadratic order of the boost velocity v. More interestingly, the relative orientation of the boost and the entangling width play a crucial role to quantify the holographic entanglement entropy in the boundary theory. The breaking of rotational symmetry in the boundary theory due to the boosting of the plasma along a specific flat direction causes this interesting feature.</p>
26.	<p><a href="#">Highly Efficient Fixation of Carbon Dioxide at RT and Atmospheric Pressure Conditions: Influence of Polar Functionality on Selective Capture and Conversion of CO<sub>2</sub></a>  R Das, CM Nagaraja - Inorganic Chemistry, 2020</p> <p><b>Abstract:</b> The rapid increase in the concentration of atmospheric carbon dioxide (CO<sub>2</sub>) has resulted in undesirable environmental issues. Hence, selective CO<sub>2</sub> capture and utilization as C1 feedstock for the preparation of high-value chemicals and fuels has been considered as a promising step toward mitigating the growing concentration of atmospheric CO<sub>2</sub>. In this direction, herein we report rational construction of a Ag(I)-anchored sulfonate-functionalized UiO-66 MOF named as MOF-SO<sub>3</sub>Ag composed of CO<sub>2</sub>-philic sulfonate functionality and catalytically active alkynophilic Ag(I) sites for chemical fixation of carbon dioxide. The MOF-SO<sub>3</sub>Ag exhibits selective as well as recyclable adsorption of CO<sub>2</sub> with a high heat of adsorption energy (Q<sub>st</sub>) of 37.8 kJ/mol. On the other hand, the analogous MOF, UiO-66 doped with Ag(I), showed a lower Q<sub>st</sub> value of 30 kJ/mol, highlighting the importance of the sulfonate group for stronger interaction with CO<sub>2</sub>. Furthermore, the MOF-SO<sub>3</sub>Ag acts as an efficient heterogeneous catalyst for cyclic carboxylation of propargylic alcohols to generate α-alkylidene cyclic carbonates in &gt;99% yield at mild conditions of RT and 1 bar CO<sub>2</sub>. More importantly, one-pot synthesis of oxazolidinones by a three-component reaction between CO<sub>2</sub>, propargylic alcohol, and primary amine has also been achieved using MOF-SO<sub>3</sub>Ag catalyst under the mild conditions. The MOF is highly recyclable and retains its superior catalytic activity even after several cycles. To the best of our knowledge, MOF-SO<sub>3</sub>Ag is the first example of MOF reported for RT chemical fixation of CO<sub>2</sub> to oxazolidinones by aminolysis of α-alkylidene cyclic carbonates under the environment-friendly mild conditions.</p>



[Histidine-Naphthalimide based Organic-Inorganic Nanohybrid for Electrochemical Detection of Cyanide and Iodide ions](#)

M Chaudhary, M Verma, KC Jena, N Singh - ChemistrySelect, 2020

27.

**Abstract:** Histidine-naphthalimide based receptors were prepared with variation of the side chain amine having morpholine and 1,1-dimethylethylenediamine. The prepared organic compounds were then employed as a framework for the fabrication of organic-inorganic nanohybrid assembly with the aim of detection of environmentally essential anions in the aqueous medium. The size and morphology of the nanohybrid particles were confirmed with TEM and DLS analysis. Hybrid nanoparticles of morpholine naphthalimide show selective and sensitive response with cyanide ion. Subsequently, the hybrid nanoparticles of 1,1-dimethylethylenediamine naphthalimide display visible difference with iodide ions and the response was electrochemically detected. Both the hybrid nanoparticles were utilized for the selective and sensitive detection of CN<sup>-</sup> and I<sup>-</sup> ions; with quite low detection limits.

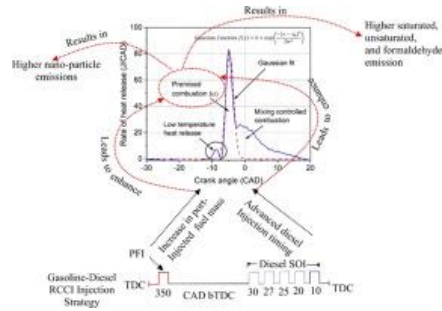
[Influence of direct injection timing and mass of port injected gasoline on unregulated and nano-particle emissions from RCCI engine](#)

MR Saxena, RK Maurya - Fuel, 2020

28.

**Abstract:** The study aims to experimentally characterize the nano-particle emissions and unregulated (i.e., saturated and unsaturated hydrocarbons and formaldehyde emissions) emissions. Present study experimentally investigates the effect of high reactivity fuel injection timings and port-injected-fuel mass on nano-particle and unregulated emissions in the gasoline-diesel RCCI engine. Additionally, empirical correlations are developed using experimental data for the estimation of particle emission characteristics. An automotive single cylinder diesel engine is modified for an in-cylinder blending of port-injection of gasoline during suction stroke and direct-injection of diesel fuel during the compression stroke. The experiments are performed on a modified engine for various diesel injection timings and port-injected gasoline mass using development electronic control unit (ECU). Nano-particle and unregulated emissions are measured using electrical mobility based particle-sizer and Fourier-transform infrared spectroscopy analyser respectively. Combustion analysis is performed by in-cylinder pressure measurement. The experimental data of nano-particle and combustion characteristics are used for the development of empirical correlation using a multivariable regression technique for determining the particle number characteristics. The parameters - premixing ratio, start of injection of diesel, and a novel parameter defined as premixed fraction of total heat release are used for the development of empirical correlations and found a good correlation for estimating the nano-particle emission characteristics. Results also indicate that advanced direct injection timing and increase in the port-injected gasoline mass leads to higher particle emissions as well as saturated, unsaturated hydrocarbon and formaldehyde emissions.

**Graphical Abstract:**



[Intestinal microbiota disruption limits the isoniazid mediated clearance of Mycobacterium tuberculosis in mice](#)

S Negi, S Pahari, H Bashir, JN Agrewala - European Journal of Immunology, 2020

29. **Abstract:** Tuberculosis (TB) continues to remain a global threat due to the emergence of drug-resistant Mycobacterium tuberculosis (Mtb) strains and toxicity associated with TB drugs. Intestinal microbiota has been reported to affect the host response to immunotherapy and drugs. However, how it affects the potency of first-line TB drug isoniazid (INH) is largely unknown. Here, we examined the impact of gut microbial dysbiosis on INH efficiency to kill Mtb. In this study, we employed in vivo mouse model, pretreated with broad-spectrum antibiotics (Abx) cocktail to disrupt their intestinal microbial population prior to Mtb infection and subsequent INH therapy. We demonstrated that microbiota disruption results in the impairment of INH-mediated Mtb clearance, and aggravated TB-associated tissue pathology. Further, it suppressed the innate immunity and reduced CD4 T-cell response against Mtb. Interestingly, a distinct shift of gut microbial profile was noted with abundance of Enterococcus and reduction of Lactobacillus and Bifidobacterium population. Our results show that the intestinal microbiota is crucial determinant in efficacy of INH to kill Mtb and impacts the host immune response against infection. This work provides an intriguing insight into the potential links between host gut microbiota and potency of INH.

[Measurement of Local Pulse Wave Velocity using Fast Ultrasound Imaging](#)

KA Singh, AK Sahani - IEEE International Symposium on Medical Measurements and Applications, 2020

30. **Abstract:** Carotid to femoral pulse wave velocity (cfPWV) is considered as the gold standard of arterial stiffness. We hypothesize that local pulse wave velocity (LPWV) may be a close surrogate of the cfPWV. Current method of measuring cfPWV is intrusive, inconvenient and requires manual measurement of carotid-femoral distance. While other measures of arterial stiffness can be done using ultrasound imaging, cfPWV required separate specialized equipment. In this paper, we provide a proof of concept of possibility of measuring LPWV on fast ultrasound frames. We used Verasonics® Vantage-256 Research ultrasound system to obtain longitudinal carotid frames at a frame rate of more than 750 frames per second. Diameter waveforms are obtained from two ends of these longitudinal frames. The minute time shift between these waveforms is used to calculate the time of flight of the waveform from one end of the carotid to other. The known distance between pixels on beamformed frames are used to calculate the LPWV. Measurements for five human volunteers were obtained which were found to statistically equal to the cfPWV measured using SphygmoCor.

[Multiband Planar Antenna for Cellular and Wireless Applications](#)


U Rafique, I Ahmad, S Agarwal, V Jain - IEEE Indian Conference on Antennas and Propagation, 2019

31.

	<p><b>Abstract:</b> A multiband planar antenna design is presented for cellular and wireless communications. The presented antenna realizes an overall size of <math>40 \times 40 \times 1.6</math> mm<sup>3</sup>. It consists of a G-shaped and inverted L-shaped radiator. The G-shaped radiator is responsible to offer 1800 MHz, 2.45 GHz, and 3.5 GHz frequency bands, while the inverted L-shaped radiator can provide resonance at 900 MHz and 5 GHz frequency bands. Moreover, the proposed multiband antenna offers good radiation characteristics and gain for desired frequency bands. The proposed antenna design is also fabricated and measured to validate the simulation results.</p>
32.	<p><a href="#"><u>Negative pressure aerosol containment box: An innovation to reduce COVID-19 infection risk in healthcare workers</u></a>  V Gupta, A Sahani, B Mohan, GS Wander – Journal of Anaesthesiology Clinical Pharmacology, 2020</p> <p><b>Abstract:</b> Healthcare workers (HCW's) are at increased risk of corona virus disease (COVID-19) infection during aerosol generating activities. The aerosol box has been used during intubation and extubation to prevent transmission of infection to HCWs. Isolation room with negative pressure has been advocated for COVID-19 patients. The described containment box has been designed to be useful in COVID intensive care unit (ICU) as a multipurpose box which is a cost effective and readily available resource. This innovation combines the containment box with negative pressure generation using central vacuum.</p>
33.	<p><a href="#"><u>Numerical Investigation of in-cylinder Tumble/swirl flow on mixing, turbulence, and combustion of Methane in SI engine</u></a>  N Yadav, MR Saxena, RK Maurya - 2020</p> <p><b>Abstract:</b> In the present study, the in-cylinder flow motion tumble/ swirl are investigated in canted valve engine and their effect on the homogeneity, turbulence, and combustion of gasoline-like fuels (Methane and Methanol) using ANSYS. The study is focused on the effect of initial swirl and tumble on the charge preparation, turbulent kinetic energy, and combustion of fuel in spark ignition (SI) engine. The flow simulation was performed in ANSYS using hybrid mesh for cold flow simulation to study the tumble/swirl flow variation, and for combustion simulation, a 2d axisymmetric model was used with initial swirl and tumble ratio for exploring the effect on premixed combustion. The flow simulation was performed for full combustion cycle to see the variation of tumble with crank position and speed. The combustion simulation was performed only for compression and power stroke to save the computational time. It is found that the flow inside the cylinder play a major role in preparation of homogeneous charge. Tumble and swirl majorly affect the turbulence, and increase in the tumble motion shifts the peak combustion pressure for few crank angle degrees earlier. Turbulent kinetic energy increases rapidly for higher swirl and tumble as the disturbance gets amplified with higher flow variations. Thus, more energy is added to the flow at TDC because of vortices added in the flow due to tumble breakdown, which leads to better mixing and combustion.</p>
34.	<p><a href="#"><u>Observation of finite-size-induced emission decay rates in self-assembled photonic crystals</u></a>  M Khokhar, RV Nair - Physical Review A, 2020</p> <p><b>Abstract:</b> We study the extent of spontaneous emission inhibition in self-assembled photonic crystals where the light path is routinely affected by unavoidable imperfections of the crystal and its finite-size. We discuss the role of finite-size effects that inadvertently modify the local density of optical states (LDOS) using time-resolved decay rate measurements from the single domains of real synthesized photonic crystals. We have obtained 34% contrast in the measured emission lifetimes at the stop gap wavelength in comparison to a wavelength</p>



	<p>outside the stop gap. We have shown a remarkable variation in the emission lifetimes at the stop gap for several domains across the sample which is nullified within a single domain. The results manifest wavelength-dependent linear scaling of lifetimes with the finite-size of the crystal domain. This is a signature of direct dependence of LDOS suppression on the crystal's finite-size which is also found to be in accordance with a recent theoretical model. The precise single-domain measurements result in a robust modification of lifetime in an otherwise weakly classified self-assembled photonic crystal.</p>
35.	<p><a href="#">On surface Modification of Ti Alloy by Electro Discharge Coating Using Hydroxyapatite Powder Mixed Dielectric with Graphite Tool</a>  G Singh, SS Sidhu, PS Bains, M Singh, AS Bhui - Journal of Bio-and Tribo-Corrosion, 2020</p> <p><b>Abstract:</b> Ti alloys from the family of metallic biomaterials are extensively used on account of their biological properties, functionality, and longevity within the human body. Due to the reactive elements such as vanadium, Ti alloys react with enzymes and body fluids causing the release of harmful ions in the body. The release of such ions promotes corrosion, bone-implant wear, and infection within the individual. However, in the recent scenario, coating of bioactive material on the substrate is one of best solution to conquer such issues. This article addresses the surface modification of medical grade Ti–6Al–4V alloy substrate with hydroxyapatite (HA) powder via Electro Discharge Coating (EDC). The experiments were performed as per Taguchi’s L8 orthogonal array considering current, pulse-on-time, pulse-off-time as input parameters. The output responses are assessed in terms of material deposition rate, surface roughness, and microhardness of coated samples. Surface morphology and phase analysis confirmed the porous texture and formation of bioactive compounds on the HA–EDC treated surface. Furthermore, in vitro wear and electrochemical corrosion behavior of the substrate and HA–EDC sample was scrutinize to analyze the improved resistance of modified surface. The results confirmed the significance of coating on substrate with improved corrosion protection efficiency (91.26%) and wear resistivity (87%) compared to untreated surface. Based on the observations, the EDC treated surface validates the surface modification offering improved bioactivity to the substrate material.</p>
36.	<p><a href="#">Oxidized graphitic carbon nitride as a sustainable metal-free catalyst for hydrogen transfer reactions under mild conditions</a>  P Choudhary, A Bahuguna, A Kumar, SS Dhankhar, CM Nagaraja... - Green Chemistry, 2020</p> <p><b>Abstract:</b> The development of green and sustainable transfer hydrogenation protocols without the use of expensive noble metals and toxic solvents is a challenging task. Herein, a highly stable, low-cost, metal-free heterogeneous catalyst, oxidized graphitic carbon nitride (O-GCN), has been developed, which exhibits efficient catalytic hydrogen transfer reactions of carbonyl compounds to corresponding alcohols under mild reaction conditions. The heterogeneous catalyst was synthesized by the chemical oxidation of graphitic carbon nitride (GCN) nanosheets, which results in the generation of carboxyl, hydroxyl and ketone groups over the GCN surface. These hydrophilic groups functionalized on the surface of O-GCN nanosheets act as catalytically active sites for the hydrogen transfer reactions of carbonyl compounds. A wide range of substrates was investigated for the hydrogen transfer reactions using 2-propanol both as a hydrogen donor and a solvent. The O-GCN nanosheets resulted in high yields and high turnover numbers (TON) demonstrating the versatile catalytic potential of the as-synthesized catalyst. The detailed optimization of the reaction parameters (temperature, time and catalyst amount) was performed, in addition to the calculation of green metric parameters. Moreover, the catalyst could be easily recovered and was used for five runs without any significant loss in catalytic activity. This study provides a green, sustainable,</p>

	attractive, and useful methodology for the hydrogen transfer reactions of a wide range of carbonyl compounds.
37.	<p><a href="#">Phase separation effects on a partially miscible viscous fingering dynamics</a> RX Suzuki, Y Nagatsu, M Mishra, T Ban - Journal of Fluid Mechanics, 2020</p> <p><b>Abstract:</b> Classical viscous fingering (VF) instability, the formation of finger-like interfacial patterns, occurs when a less viscous fluid displaces a more viscous one in porous media in immiscible and fully miscible systems. However, the dynamics in partially miscible fluid pairs, exhibiting a phase separation due to its finite solubility into each other, has not been largely understood so far. This study has succeeded in experimentally changing the solution system from immiscible to fully miscible or partially miscible by varying the compositions of the components in an aqueous two-phase system (ATPS) while leaving the viscosities relatively unchanged at room temperature and atmospheric pressure. Here, we have experimentally discovered a new topological transition of VF instability by performing a Hele-Shaw cell experiment using the partially miscible system. The finger formation in the investigated partially miscible system changes to the generation of spontaneously moving multiple droplets. Through additional experimental investigations, we determine that such anomalous VF dynamics is driven by thermodynamic instability such as phase separation due to spinodal decomposition and Korteweg convection induced by compositional gradient during such phase separation. We perform the numerical simulation by coupling hydrodynamics with such chemical thermodynamics and the spontaneously moving droplet dynamics is obtained, which is in good agreement with the experimental investigations of the ATPS. This numerical result strongly supports our claim that the origin of such anomalous VF dynamics is thermodynamic instability.</p> 
38.	<p><a href="#">Pole-Zero Analysis of a simple Gate Driver Circuit over the medium range of frequency used in Power Electronics Devices</a> S Meikap, KR Sekhar - IEEE Applied Power Electronics Conference and Exposition, 2020</p> <p><b>Abstract:</b> In recent, high frequency power converters are more popular due to extensive use in electric vehicle and micro grid applications. In high frequency power converters PCB designing is an important part of the circuit designing specially for high-frequency operation. In all power electronics systems, PCB is used for compact circuits but the effect of parasitic elements in the PCB is usually neglected. While designing the gate driver circuit for high-frequency operation devices requires proper characterization of the PCB parasitic element along with the other resistive and capacitive elements used. Even in lower frequencies if the parasitic elements not considered creates ripples in the output. The paper presents a detailed pole-zero analysis of a simple gate driver circuit and the effect of different frequency operations on the same design to represent the need for different values of external resistor and capacitor to get the best voltage waveform to feed the gate terminal of the power device.</p>
39.	<p><a href="#">Potential Applications of SCATSAT-1 Satellite Sensor: A systematic review</a> S Singh, RK Tiwari, HS Gusain, V Sood - IEEE Sensors Journal, 2020</p>

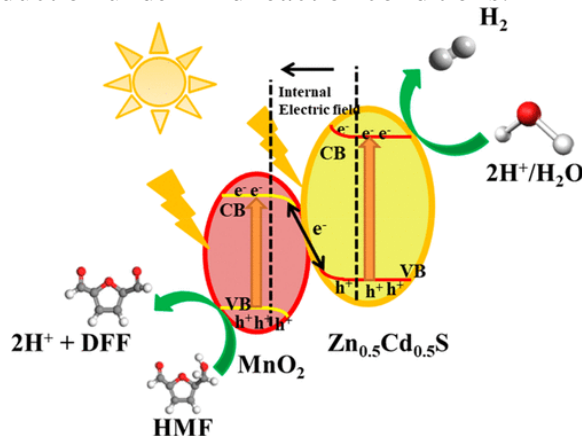
	<p><b>Abstract:</b> The Ku-band (13.5 GHz) based scatterometer is the main sensor onboard Scatterometer Satellite (SCATSAT-1) launched on 26th September 2016 by Indian Space Research Organization (ISRO). The SCATSAT-1 satellite sensor provides daily updates on the conditions of atmospheric, oceanographic, agriculture and cryospheric parameters. Moreover, it delivers data products (Level 1–4) in form of different parameters (Sigma-naught <math>\sigma_0</math>, Gamma-naught <math>\gamma_0</math>, brightness temperature BT, wind vectors and velocity) at two different polarization modes (HH and VV). Since launch, several studies have been carried out to explore the potential of SCATSAT-1 satellite sensor for remote observation of the ocean as well as the land surface at the global level. Besides the conventional applications in weather and oceanic domains which are based on wind vector data, emerging applications over land use and land cover are also introduced. This paper aims to address the current status of SCATSAT-1 applications in different scientific domains such as oceanographic, cryospheric, agriculture and land hydrology. It is expected that such an extensive exploration of the applications of SCATSAT-1 satellite sensor will provide important insights for future utilization of scatterometer data.</p>
40.	<p><a href="#"><u>Prioritized S-ALOHA for URLLC</u></a>  <a href="#"><u>S Pandey, K Shandilya, S Agarwal - International Wireless Communications and Mobile Computing, 2020</u></a></p> <p><b>Abstract:</b> Ultra reliable low latency communication (URLLC) is one of the main goals in 5G. URLLC requires highly reliable and low latency transmission of safety critical and control packets. Slotted ALOHA forms one of the widely used access schemes in cellular communication. In this paper, we study the performance of URLLC packet transmissions utilizing slotted ALOHA and propose a prioritized access mechanism to provide low latency and high reliability transmission of delay critical packets. We consider two types of traffic, namely, regular traffic and URLLC traffic. URLLC packets have stringent delay requirements, thus, they are provided high priority access to the channel. Via analytical formulation, we obtain the packet delay distribution function for both URLLC and regular packets and formulate an optimization problem to maximize the reliability of regular packets given that the URLLC packets meet their required reliability threshold. Results show that by enabling prioritized access to URLLC packets, their reliability requirements can be met, while at the same time, regular packet transmission can make most use of the remaining channel.</p>
41.	<p><a href="#"><u>Quality of Service Driven Resource Allocation in Network Slicing</u></a>  <a href="#"><u>S Saibharath, S Mishra, C Hota - IEEE 91st Vehicular Technology Conference, 2020</u></a></p> <p><b>Abstract:</b> Network slices are counted as key technology enablers to provide tailored services and isolation for different Fifth Generation (5G) cellular network application instances. A network slice is an independent end-to-end logical network over a shared physical substrate network, capable of providing a specific set of negotiated services to the customers, quite analogous to virtual machines offered in the domain of cloud computing. In this paper, we perform a systematic study of allocation and dynamic on-demand provisioning of network resources for the slices. The core parameters of Quality of Experience (QoE) to end-user systems, Network performance, and Operating efficiency are carefully applied while placing network virtual functions and determining the nodes, links, and resources for assignment to these slices. Network slices are expected to provide end-to-end capabilities while providing customized offerings. Slices can be further divided into various categories such as RAN, Transport and Core network slices. Our work examines the allocation of the above categories as independent sub-problems and latter amalgamate it into an end-to-end multi-objective constrained optimization problem. Our proposed approach is influenced by Multiple Attribute</p>

	Decision Making, Analytical Hierarchy Processing for slice assignment and enhanced Dinic's Maximum Flow Method to find all possible virtual paths for allocations. Simulations are carried out through NS3 and results are compared against well-known algorithms.
42.	<p><a href="#">Quasi-elastic scattering measurements of the <math>^{28}\text{Si} + ^{142}\text{Nd}</math> system at back-angle</a> S Biswas, A Chakraborty, A Jhingan, D Arora...RN Sahu... - Indian Journal of Pure &amp; Applied Physics, 2020</p> <p><b>Abstract:</b> The barrier distribution of a system can be extracted from excitation function data obtained either through fusion reaction or through quasi-elastic scattering measurement. In the present work, the quasi-elastic excitation function has precisely been measured at back angle for the <math>^{28}\text{Si} + ^{142}\text{Nd}</math> system at energies around the Coulomb barrier and the corresponding experimental barrier distribution has been extracted. The experimental data has been interpreted in the frame work of the coupled channel calculations which include couplings to different possible modes of excitations of the interacting target-projectile combination. The possible effect of the nature of projectile excitations on the derived barrier distribution has been presented.</p>
43.	<p><a href="#">Reading a Feminist Epistemology in Margaret Atwood's MaddAddam</a> R Ringo, J Sharma - ELOPE: English Language Overseas Perspective and Enquiries, 2020</p> <p><b>Abstract:</b> This paper proposes an epistemological interpretation of Margaret Atwood's MaddAddam (2013). Set in a post-anthropocene world, Atwood's biopunk work indicates the rise of posthumanism after the "Waterless Flood" that proves apocalyptic. This interpretation is attempted through emphasis on the protagonist Toby's practice of epistemic writing and her art of storytelling. Divided into two major sections, the article illustrates a revival of an epistemological feminist subculture. The first section discusses the significance of a feminist standpoint in unravelling posthuman reality. It describes Toby's epistemological endeavor to enlighten the Crakers and enrich their bioengineered minds with the story of their creation. The second section builds upon the idea of bisexual writing and Toby as its prime progenitor and practitioner. The conclusion remarks on the relevance of feminist epistemology in integrating the two communities in the post-anthropocene.</p>
44.	<p><a href="#">Secrecy Analysis of MRC Diversity Schemes over Nakagami-m Fading Channels</a> HK Sharma, B Kumbhani - IEEE International Conference on Advanced Networks and Telecommunications Systems, 2019</p> <p><b>Abstract:</b> In this paper, we analyze the secrecy performance of maximal ratio combining (MRC) diversity scheme over Nakagami-m fading channels. Closed form expressions for probability of existence of positive secrecy (PEPS) and lower bound on secrecy outage probability (SOP) are derived. We also analyse the secrecy diversity order of the system and concluded that the secrecy diversity order is <math>m M</math>. The derived expressions are validated by the results obtained from Monte Carlo simulations. The lower bound on SOP evaluated from the derived expressions are found accurately tight from the excellent agreement between analytical and simulation results.</p>
45.	<p><a href="#">Signatures of non-trivial band topology in LaAs/LaBi heterostructure</a> P Wadhwa, TJD Kumar, A Shukla, R Kumar - Journal of Physics: Condensed Matter, 2020</p> <p><b>Abstract:</b> In this article, we investigate non-trivial topological features in a heterostructure of extreme magnetoresistance (XMR) materials LaAs and LaBi using density functional theory. The proposed heterostructure is found to be dynamically stable and shows bulk band inversion with non-trivial <math>Z_2</math> topological invariant and a Dirac cone at the surface. In addition, its electron and hole carrier densities ratio is also calculated to investigate the possibility to</p>

	possess XMR effect. Electrons and holes in the heterostructure are found to be nearly compensated, thereby facilitating it to be a suitable candidate for XMR studies.
46.	<p><a href="#">Spectrally selective modification in the emission lifetimes of nitrogen vacancy centers in nanodiamonds</a> S Sharma, RV Nair - <i>Journal of Optics</i>, 2020</p> <p><b>Abstract:</b> The nitrogen-vacancy (NV) center is one of the most prominent candidates for quantum technologies, and its efficient utilization requires control over its spontaneous emission rate. Here, we report the wavelength-selective enhancement and suppression of NV center emission lifetime at room temperature by modifying the local density of optical states around them. The results are explained using the Barnett-Loudon sum rule and also supported by the LDOS calculations. Two complementary measurement geometries are employed to study the direction-dependent emission behavior from the nanodiamonds decorated on the top of photonic crystals. The lifetime distributions are compared with a proper reference sample using the Kolmogorov-Smirnov test to verify the distinct nature of lifetime distributions. The wavelength-selective enhancement or suppression of emission rates would be useful for NV center-based high-resolution imaging and effective readout of its charge states.</p>
47.	<p><a href="#">Sputtered-growth of high-temperature seed-layer assisted <math>\beta</math>-Ga<sub>2</sub>O<sub>3</sub> thin film on silicon-substrate for cost-effective solar-blind photodetector application</a> K Arora, M Kumar - <i>ECS Journal of Solid State Science and Technology</i>, 2020</p> <p><b>Abstract:</b> <math>\beta</math>-Ga<sub>2</sub>O<sub>3</sub> thin films was grown on cost-effective p-Si(100) substrate by sputtering technique. The evolution of crystalline structure with growth parameters revealed that the gallium oxide thin film grown on the high-temperature seed layer and various optimised growth parameters like sputtering power, deposition pressure and pre-substrate annealing has been proved extremely beneficial in exhibiting excellent crystalline quality. However, the direct growth of <math>\beta</math>-Ga<sub>2</sub>O<sub>3</sub> on Si substrate with seed-layer was found to be amorphous in nature. The discussion about the critical role of varied growth conditions were carried in detail. The photoresponse of the optimized device showed a photoresponsivity of 95.64 AW<sup>-1</sup> and a corresponding quantum efficiency of <math>4.73 \times 10^4</math> % at moderate bias under 250 nm illumination which is higher than most of the devices being reported on planar <math>\beta</math>-Ga<sub>2</sub>O<sub>3</sub> solar-blind photodetectors deposited on high cost substrates. Moreover, the device showed the high transient response at moderate as well as at self-bias mode with good reproducibility and stability. The rise and decay time of the photodetector at self-powered mode was found to be in millisecond (58.3 ms/34.7 ms). This work paves the alternative way towards the fabrication of <math>\beta</math>-Ga<sub>2</sub>O<sub>3</sub> solar-blind photodetector on cost-effective substrate and compatible with mature Si technology.</p>
48.	<p><a href="#">Visible-light-driven selective oxidation of biomass-derived HMF to DFF coupled with H<sub>2</sub> generation by noble metal-free Zn<sub>0.5</sub>Cd<sub>0.5</sub>S/MnO<sub>2</sub> heterostructures</a> S Dhingra, T Chhabra, V Krishnan, CM Nagaraja - <i>ACS Applied Energy Materials</i>, 2020</p> <p><b>Abstract:</b> The development of efficient photocatalysts for utilization of solar energy for water splitting coupled with oxidation of biomass-derivatives is of utmost importance for the simultaneous production of clean fuel (H<sub>2</sub>) and value-added chemicals. Consequently, herein we report the development of the Z-scheme photocatalytic system, Zn<sub>0.5</sub>Cd<sub>0.5</sub>S/xMnO<sub>2</sub>, which has the optimum band structure suitable for efficient visible-light-assisted photocatalytic H<sub>2</sub> generation integrated with selective oxidation of biomass-derived 5-hydroxymethylfurfural (HMF) to a more value-added product, 2,5-diformylfuran (DFF). The electron microscopy analyses of the samples revealed the presence of Zn<sub>0.5</sub>Cd<sub>0.5</sub>S</p>

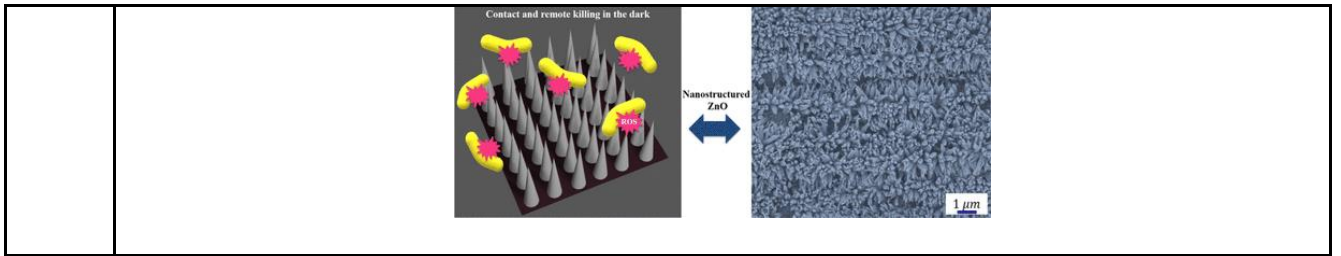


microspheres composed of smaller nanocrystals with the surface covered by the MnO<sub>2</sub> nanostructure and the intimate contact between Zn<sub>0.5</sub>Cd<sub>0.5</sub>S and MnO<sub>2</sub>. Photocatalytic investigations revealed the highest activity for Zn<sub>0.5</sub>Cd<sub>0.5</sub>S/1%MnO<sub>2</sub>, affording a DFF yield of 46% and a simultaneous H<sub>2</sub> generation rate of 1322 μmol g<sup>-1</sup> in 24 h, which are, respectively, 9 and 4 times higher than those of parent sample, Zn<sub>0.5</sub>Cd<sub>0.5</sub>S. Further, the best heterostructure exhibits good catalytic activity even under natural sunlight irradiation, affording DFF with a 14% yield and H<sub>2</sub> generation rate of 152.6 μmol g<sup>-1</sup> in 6 h. The high catalytic activity of the heterostructure over the parent materials has been attributed to efficient separation of photogenerated charge-carriers with the aid of the Z-scheme mechanism and the synergistic catalysis between Zn<sub>0.5</sub>Cd<sub>0.5</sub>S and MnO<sub>2</sub>. Overall, this work represents a unique demonstration of noble metal-free selective oxidation of HMF to DFF integrated with H<sub>2</sub> production under mild reaction conditions.



[Water-based Scalable Methods for Self-Cleaning Antibacterial ZnO-Nanostructured Surfaces](#)  
 A Millionis, A Tripathy, M Donati, CS Sharma, F Pan... - *Industrial & Engineering Chemistry Research*, 2020

49. **Abstract:** Bacterial colonization poses significant health risks, such as infestation of surfaces in biomedical applications and clean water unavailability. If maintaining the surrounding water clean is a target, developing surfaces with strong bactericidal action, which is facilitated by bacterial access to the surface and mixing, can be a solution. On the other hand, if sustenance of a surface free of bacteria is the goal, developing surfaces with ultralow bacterial adhesion often suffices. Here we report a facile, scalable, and environmentally benign strategy that delivers customized surfaces for these challenges. For bactericidal action, nanostructures of inherently antibacterial ZnO, through simple immersion of zinc in hot water, are fabricated. The resulting nanostructured surface exhibits extreme bactericidal effectiveness (9250 cells cm<sup>-2</sup> h<sup>-1</sup>) that eliminates bacteria in direct contact and also remotely through the action of reactive oxygen species. Remarkably, the remote bactericidal action is achieved without the need for any illumination, otherwise required in conventional approaches. As a result, ZnO nanostructures yield outstanding water disinfection of >99.98%, in the dark, by inactivating the bacteria within 3 h. Moreover, Zn<sup>2+</sup> released to the aqueous medium from the nanostructured ZnO surface have a concentration of 0.73 ± 0.15 ppm, markedly below the legal limit for safe drinking water (5–6 ppm). The same nanostructures, when hydrophobized (through a water-based or fluorine-free spray process), exhibit strong bacterial repulsion, thus substantially reducing bacterial adhesion. Such environmentally benign and scalable methods showcase pathways toward inhibiting surface bacterial colonization.



**Disclaimer:** This publication digest may not contain all the papers published. Library has compiled the publication data as per the alerts received from Scopus and Google Scholar for the affiliation “Indian Institute of Technology Ropar” for the month of July 2020. The author(s) are requested to share their missing paper(s) details if any, for the inclusion in the next publication digest.